

# Optimal Control of a Mackerel-Mimicking Robot for Energy Efficient Trajectory Tracking

Seunghee Lee<sup>1</sup>, Jounghyun Park<sup>1</sup>, Cheolheui Han<sup>2</sup>

1. Department of Mechanical Engineering Hanyang University, Seoul 133–791, Korea

2. Department of Aeronautical and Mechanical Design Engineering, Chungju National University,  
Chungju 380–702, Korea

---

## Abstract

A robotic fish, BASEMACK1, is designed and fabricated by mimicking the shape of a live mackerel. Three DC servo-motors are serially linked together and actuated to mimic the mackerel's Carangiform motion. Hydrodynamic characteristics of a fish-mimetic test model are experimentally identified and utilized in order to numerically simulate fish swimming. The discrete set of kinematic and dynamic parameters are obtained by considering required horizontal and lateral forces and minimum energy consumption. Using the optimized parameter set, optimal control of the robot is studied.

**Keywords:** mackerel-mimicking robot, optimal control, trajectory tracking

Copyright © 2007, Jilin University. Published by Elsevier Limited and Science Press. All rights reserved.

---

## 1 Introduction

Creatures in nature have evolved to survive the harsh environmental changes and strong competitions for limited space and food resources, adapting or morphing their outward appearance and their component parts. In 1936, Gray estimated the muscle power required by a dolphin and the power for a dolphin-shape body to move through the water and found that the required power for the dolphin-shape body is seven times larger than that of a live dolphin<sup>[1]</sup>. Since then, scientists and engineers have been enticed to reveal the relationship between the fish's swimming behavior and their fascinating swimming agility with high performance<sup>[2]</sup>.

Triantafyllou *et al.*<sup>[3]</sup> showed that the fast-swimming fish adopts the flexible tail fin motion in order to obtain high performance by controlling the vorticity, minimizing the energy lost in the wake. It was verified by showing that a tuna-mimicking robot, "RoboTuna" achieved significant drag reduction using the flexible oscillating mechanical devices. With recent progresses in smart materials and microelectro- mechanical-

systems (MEMS) technology, there have been increasing efforts toward developing fish-mimetic robots or underwater vehicle by using fish-mimetic propulsors<sup>[4,5]</sup>.

Tuna can swim at high speed with high efficiency. The study of tuna can lead to the development or improvement of the aquatic man-made vehicles or robots. Eel-mimicking robot can be utilized to swim in narrow spaces. For a small-size vehicle less than a whale, undulation-based propulsion can be more efficient than the conventional propeller-based propulsion. The former is less noisy and more maneuverable than the latter. The fish-mimetic robots might be used in many marine and military fields such as exploration of fish behavior, detecting leaks in oil pipelines, seabed exploration, mine countermeasures and robotic education, *etc.*<sup>[6]</sup>.

Any current mechanical or electrical system can not have the exactly same functions as bio-organics systems existing in nature. Thus, the mechanical system should be so designed or controlled as to be adapted to the given environment. In this paper, an optimal motion pattern of a fish-mimetic robot is studied as an initial stage to intelligent control of the robot. A mackerel-mimetic robot

---

**Corresponding author:** Cheolheui Han

**E-mail:** [chhan@cjnu.ac.kr](mailto:chhan@cjnu.ac.kr)

fish (BASEMACK1: Biomimetics and Aircraft System Engineering laboratory MACKerel 1) is fabricated and used as a test model for a fluid-dynamic study. Hydrodynamic characteristics of the robot fish are measured in a water-tank. Using the measured hydrodynamic coefficient data, a hydrodynamic model of the robot fish is established. The optimized motion parameter set with minimum energy consumption is obtained using the numerical simulation results and measured data. Then, a numerical simulation is done to investigate the adaptation capability of the robotic fish to the given environment.

## 2 Fabrication and test-rig setup

Fig. 1 shows the robotic fish (BASEMACK1) that is fabricated by mimicking the shape of a live mackerel. Serially-linked three DC servo-motors are actuated to mimic the mackerel's carangiform motion. A DC servo motor weighs 66g. Its maximum torque and speed are 102 N·cm and 7 rad·s<sup>-1</sup> for unloaded condition, respectively. Water is critically harmful to the normal operation of electric motors and devices. The core electrical parts are covered with latex film for waterproof. Then, the outer shape of BASEMACK1 is formed with silicon using a casting method.

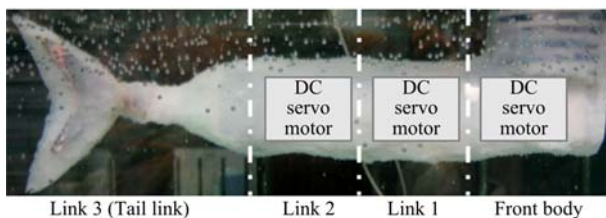


Fig. 1 Fabricated BASEMACK1.

Fig. 2 shows the experimental setup for measuring the hydrodynamic characteristics of the fish-mimicking robot. To identify the hydrodynamic characteristics of the robotic fish, forces and torques are measured by using a 6-axis force/torque sensor. One side of the 6-axis force/torque sensor is fixed to the base plate which is also clamped to water tank. Another side of the sensor is attached to an aluminum rod. The diameter of the rod is 30mm that is thick enough to prevent the possible distortion due to the forces generated by the fish robot. The front body of the BASEMACK1 is firmly attached to the rod. The tail fin is made of a 1 mm thick flexible metal plate. The total length of the BASEMACK1 is 320 mm. The body weight is 0.53 kg. The size of the water tank is 1530 × 420 × 600 (Length × Width × Height, mm). The distance from the floor of the water tank to the center of gravity of the BASEMACK1 is 300 mm. The height of water in the water tank is 500 mm. Free surface can affect the hydrodynamic characteristics of the robot fish. Thus, the robot fish is fully submerged into the water. Measured data from the 6-axis force/torque sensor is transferred via DAQ board to a computer. An in-house application program (Robot Fish Manipulation Code, RFMC) is developed in order to control the motions of the links and to gather the necessary data. The RFMC communicates with DC servo motors through a USB2RS485 communication system. The RFMC allocates a desired trajectory command to each servo motor. Then, each motor follows the given trajectory command and returns its resultant trajectory and motor current information back to the application program.

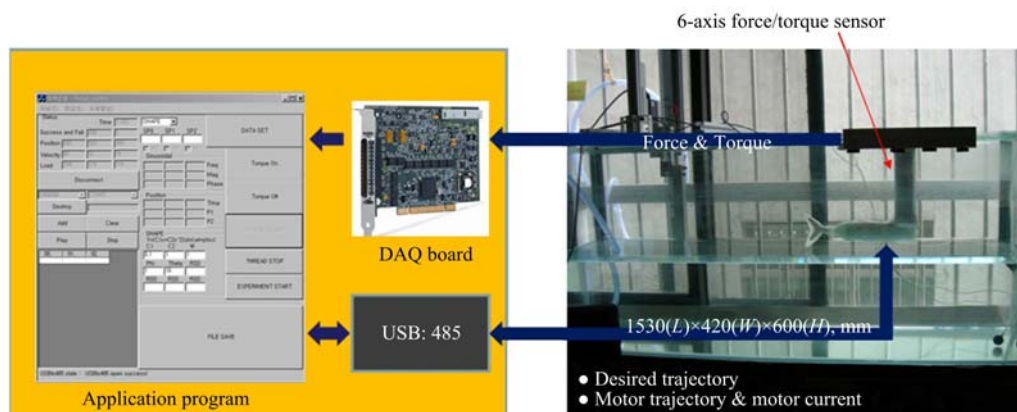


Fig. 2 Experimental setup.

### 3 Kinematics

Two coordinate systems are used to describe the unsteady motions of fish-mimicking robot moving through stationary fluid medium (see Fig. 3). One is a water-tank-fixed coordinate system and the other is a fish-fixed coordinate system. In the figure,  $v_c$  and  $v_{\text{water}}$  represent the velocity of the body and the velocity of the flow coming to the robot fish, respectively. It is assumed that the water is stationary ( $v_{\text{water}} = 0.0$ ). The relative velocity between the water and the tail fin for the numerical simulation is defined as the velocity of a quarter-chord point of the root chord ( $v_p$ ) in the tail fin.

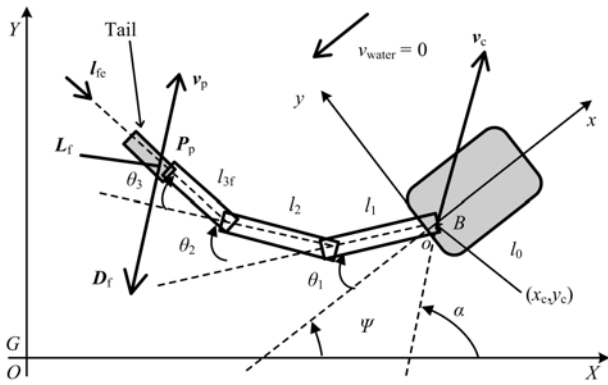


Fig. 3 Nomenclature of the robot fish kinematics.

The position of the quarter chord point in the tail fin with respect to the body-fixed frame is a function of relative angles among three links. In the following notations, the physical and geometrical properties with respect to the body fixed frame are represented with superscripted prime, for example  $x'_p$ .

The position of the quarter chord point in the tail can be written as

$$\mathbf{P}'_p = \begin{bmatrix} x'_p \\ y'_p \end{bmatrix} = \begin{bmatrix} -l_1 c(\theta_1) - l_2 c(\theta_1 + \theta_2) - l_{3f} c(\theta_1 + \theta_2 + \theta_3) \\ l_1 s(\theta_1) + l_2 s(\theta_1 + \theta_2) + l_{3f} s(\theta_1 + \theta_2 + \theta_3) \end{bmatrix}, \quad (1)$$

where both  $c(x)$  and  $s(x)$  are the abbreviations of  $\cos(x)$  and  $\sin(x)$ , respectively. The velocity of the position of the quarter chord point in the tail fin is given by

$$\bar{\mathbf{v}}'_p = \frac{d}{dt}(\mathbf{P}'_p). \quad (2)$$

The velocity in the water-tank-fixed frame is given by

$$\bar{\mathbf{v}}_p = R_G^B \bar{\mathbf{v}}'_p + \frac{d}{dt}(R_G^B) \mathbf{P}'_p, \quad (3)$$

The Carangiform motion of both the rear part of the robot fish body and the tail fin can be represented as a Body Shape Function (BSF)<sup>[7]</sup>.

$$y(x, t) = (C_1 x + C_2 x^2) \sin(2\pi f t + \phi x) \quad (4)$$

In Eq. (4),  $C_1$  and  $C_2$  are the coefficients of linear incremental term and the second order incremental term, respectively,  $f$  is the oscillatory frequency and  $\phi$  indicates the body wave number.

In order to implement BSF to a robotic fish, Yu<sup>[8]</sup> determined the angle of each link in order to have minimum integrating error with BSF in offline. In our research, real time transformation from BSF directly to link angles is accomplished by using the following equations

$$\begin{cases} \theta_1(t) = a \tan 2(y(l_1, t), l_1) \\ \theta_2(t) = a \tan 2(y(l_1 + l_2, t) - y(l_1, t), l_2) - \theta_1(t) \\ \theta_3(t) = a \tan 2(y(l_1 + l_2 + l_3, t) - y(l_1 + l_2, t), l_2) - \theta_2(t) - \theta_1(t). \end{cases} \quad (5)$$

### 4 Hydrodynamic characteristics

Following the notations of Mason<sup>[9]</sup> and Yu<sup>[10]</sup>, lift force ( $\mathbf{L}_f$ ) and drag force ( $\mathbf{D}_f$ ) of the tail fin can be represented as following equations,

$$\mathbf{L}_f = \pi \rho_f l_f d (\bar{\mathbf{v}}'_p \times \bar{\mathbf{l}}_{fe}) \times \bar{\mathbf{v}}'_p, \quad (6)$$

$$\mathbf{D}_f = -2\pi \rho_f l_f^2 \bar{\mathbf{v}}'_p \frac{\|\bar{\mathbf{v}}'_p\|^2 - (\bar{\mathbf{v}}'_p \cdot \bar{\mathbf{l}}_{fe})^2}{\|\bar{\mathbf{v}}'_p\|}, \quad (7)$$

where  $\rho_f$  is water density,  $l_f$  is the distance between the leading edge of the fin to the quarter-chord point.  $\bar{\mathbf{l}}_{fe}$  is a unit tangential vector to the tail fin and  $d$  is a span of tail fin. Lift and drag forces exerted on each link in the global coordinates are

$$\mathbf{D}_i = C_{Di} \bar{\mathbf{v}}'_i \frac{\|\bar{\mathbf{v}}'_i\|^2 - (\bar{\mathbf{v}}'_i \cdot \bar{\mathbf{l}}_{ie})^2}{\|\bar{\mathbf{v}}'_i\|}, \quad (8)$$

$$\mathbf{L}_i = C_{Li} (\bar{\mathbf{v}}'_i \times \bar{\mathbf{l}}_{ie}) \times \bar{\mathbf{v}}'_i, \quad (9)$$

where  $C_{Di}$  and  $C_{Li}$  is the lift and drag coefficients.

In case when the fish-mimicking robot is stationary, the relative velocity of the body surface to water is small.

Then the most of hydrodynamic forces are generated from the tail fin. In the numerical simulation, it is assumed that the mass/inertia of the front body is infinite and the fish-mimicking robot remains stationary. The numerical simulation is performed by following the roadmap in Fig. 4. The hydrodynamic forces are calculated by considering the trajectory of each motor and the rotation of the body. When the initial state of the body rotation is known, the next state of the rotation of the body can be easily calculated using the estimated torque which is a function of the hydrodynamic forces exerted on the tail fin.

To get a BSF parameter set that produces the maximum propulsion force, experiments were performed by changing the motion parameters such as  $C_1$ ,  $C_2$  and  $\omega$ . Fig. 5 shows the comparison between the computed results and measured data. The last link (where the tail fin is connected) is manipulated to change its angle as an assigned sinusoidal function,  $\theta_3 = 0.35 \sin(6.6\pi t)$ . The angles of the other links are all set to zero. Using Eqs. (8) and (9), the hydrodynamic coefficients of

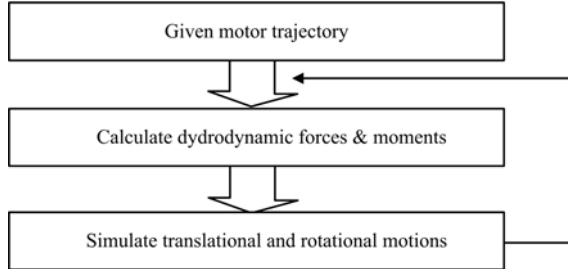


Fig. 4 Roadmap of the present numerical simulation.

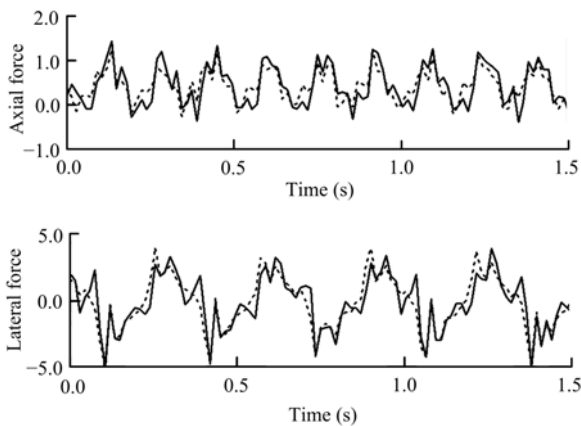


Fig. 5 Comparison between the computed and measured hydrodynamic forces (solid line: measured data, dashed line: estimated).

the robot fish are estimated as  $C_{Df} = 12.3$  and  $C_{Lf} = 4.1$ . A numerical simulation is performed to check the validity of the present method. It is shown in Fig. 5 that the simulated results are in good agreement with the measured data.

Fig. 6 shows the time-averaged propulsion force for the change in the Strouhal number ( $St = fA/U$ ), where  $A$  is the averaged total lateral excursion of the tail fin at its junction to the front body, and  $U$  is the forward speed of the robotic fish. In the figure, the estimated hydrodynamic coefficients are in good agreement with the measured data. Thus, it can be said that the numerical simulation sufficiently represents the real system. It is also found that the time-averaged propulsion force is a quadratic polynomial function of the Strouhal number ( $F_x \sim St^2$ ). Thus, the time-averaged propulsion force with low-energy consumption can be approximated as

$$\langle F_x \rangle = K_{Fx} St^2, \quad (10)$$

where  $K_{Fx}$  is the propulsion coefficient.

Fig. 7 shows the simulated values of the BSF parameters with which the fish-mimicking robot can generate the given propulsion force. During the simulation, the rotational effect of the front body is considered. The moment of inertia is set to be  $0.03 \text{ kg}\cdot\text{m}^2$ . The range of the parameters are set as  $C_1$  (0.1~0.3),  $C_2$  (0.1~2.0), and  $f$  (0.1~2.0). Within the given range of the propulsion force, the changes of  $C_1$  and  $C_2$  are insignificant whereas the changes of frequency are significant. The values of the propulsion coefficient for the robot fish with low-energy consumption is nearly constant ( $K_{Fx} = 0.504$ ) when  $F_x > 0.05 \text{ N}$ . When the front body is fixed with no

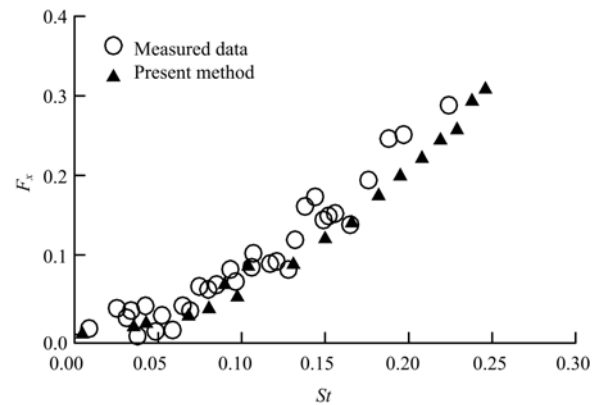


Fig. 6 Time-averaged propulsion force with the change in the Strouhal number.

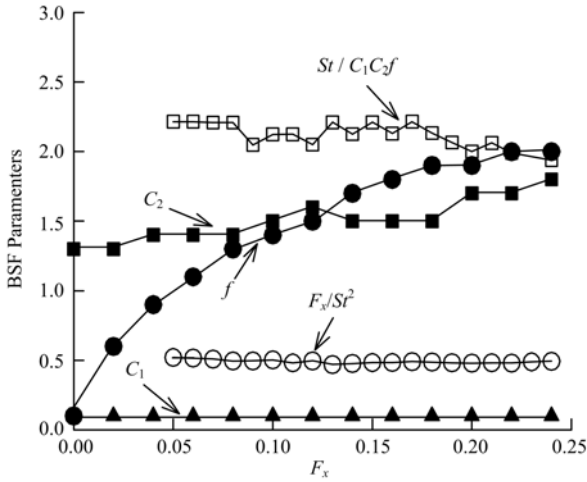


Fig. 7 Optimized BSF parameters, propulsion and Strouha number coefficients with which the fish-mimicking robot can produce the equal propulsion force.

rotational motion, Strouhal number can be calculated directly by using the values of the BSF parameters. When the front body rotates, Strouhal number should be calculated by considering the rotation of the front body. The change of the Strouhal number coefficient due to the variation of time-averaged propulsion force can be defined as

$$K_{St} = \frac{St}{C_1 C_2 f} . \quad (11)$$

From Fig. 7, it is found that the average value of  $K_{St}$  is 2.045. From Eqs. (10) and (11), the frequency of the fish-mimicking robot with minimum energy consumption can be represented as a function of averaged propulsion force

$$f = \sqrt{\frac{\langle F_x \rangle}{K_{fx}}} \frac{1}{K_{St} \bar{C}_1 \bar{C}_2} , \quad (12)$$

where both  $\bar{C}_1$  and  $\bar{C}_2$  are the optimized values of  $C_1=0.1$  and  $C_2=1.5$ , respectively.

Fig. 8 shows the optimal frequency with which the fish-mimicking robot can produce the equal propulsion force with minimum energy consumption. It is found that the optimal frequency is approximately proportional to the square root of the required propulsion force. By using the obtained frequency values for generating the propulsion force with the minimum energy consumption, it is possible to have the fish-mimicking robot follow the given trajectory.

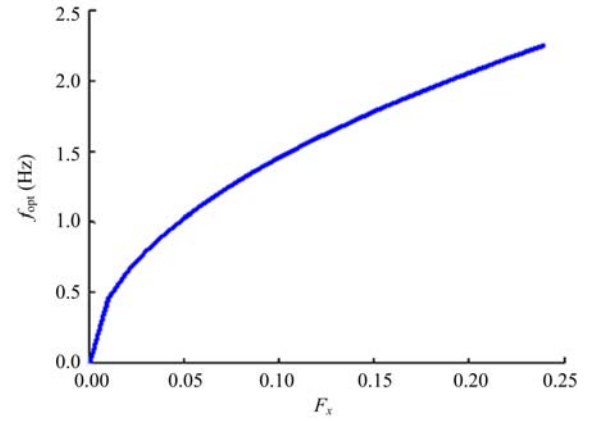
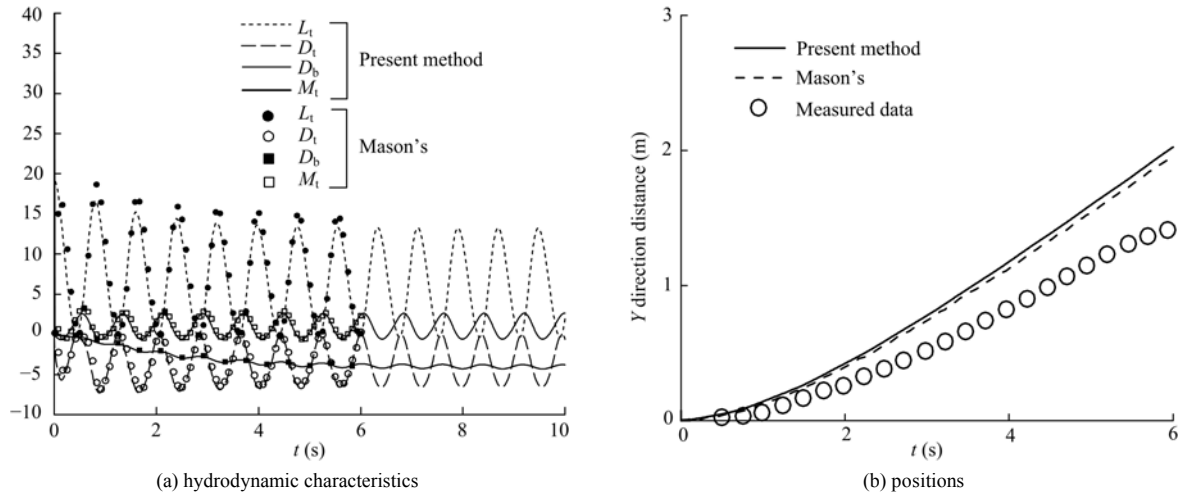


Fig. 8 Optimal frequency with which the fish-mimicking robot can produce the equal propulsion force with minimum energy consumption.

## 5 Simulation

A simulator is developed in order to design and verify the controllers of the BASEMACK1 using SimMechanics (MATHEWORKS). To validate the simulator, the present simulator uses the information on the added mass, lift and drag coefficients of Mason's simulation<sup>[9]</sup>. Fig. 9a and b shows the simulated hydrodynamic characteristics and positions. During the simulation, the body is assumed to move forward without any rotation angle as in Mason's simulation. It is found that the present method agrees well with Mason's simulator. The slight discrepancy between the results is mainly due to the input difference (Mason used the actual joint angle trajectories whereas our simulator a desired sinusoidal function of joint angle is taken as input).

Fig. 10 and Fig. 11 show the simulated results using the data of a Mackerel-mimicking robot. The hydrodynamic coefficients of the tail are used for the present Mackerel-mimicking robot ( $C_{Df}=12.3$  and  $C_{Lf}=4.1$ ). Body drag coefficient for the present model is obtained by using Mason's experimental results with the scaling factor of 0.23. In the present study, the rotation of the body is allowed during the simulation, which results in slight movement of the position of the fish body in  $y$  direction. Fig. 11 represents the hydrodynamic characteristics of the fish-mimicking body and its movement. As shown in Fig. 11, the position of the body in  $y$  direction is biased as designated by the controller, which shows the possible control of the rotation of the body.



**Fig. 9** Validation of present simulator with Mason's,  $\phi_1 = 0.6\sin(4.0t)$ ,  $\phi_2 = 0.3\sin(4.0t - \pi/3)$ .

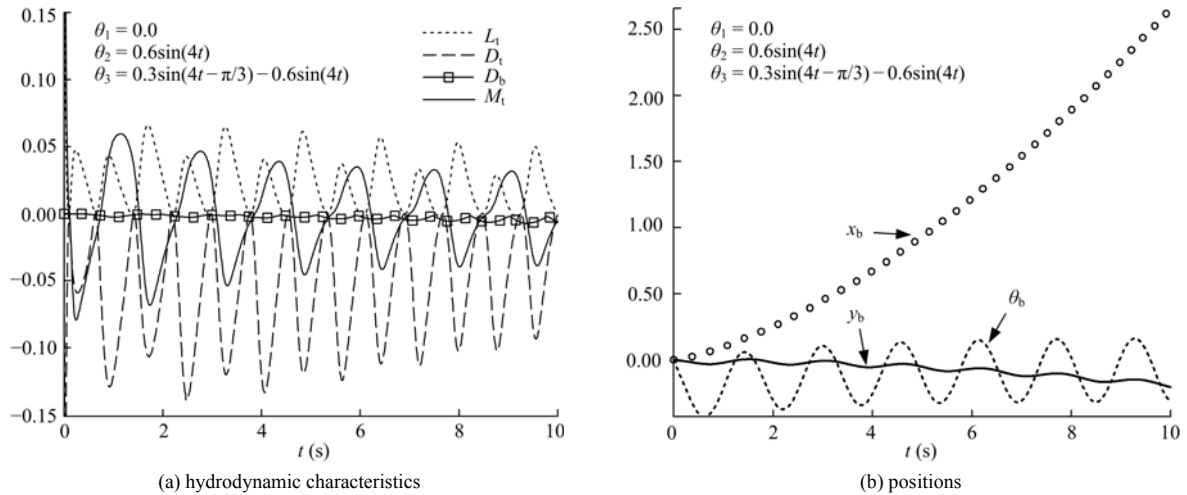


**Fig. 10** Simulation using the data of a Mackerel-mimicking robot without body rotation model,  $\phi_1 = 0.6\sin(4.0t)$ ,  $\phi_2 = 0.3\sin(4.0t - \pi/3)$ .

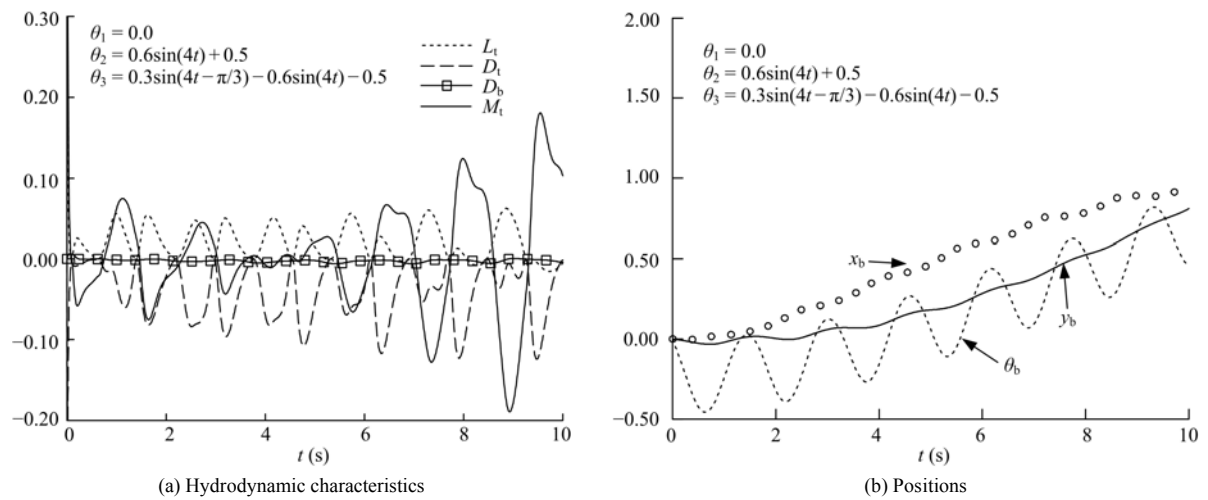


**Fig. 11** Simulation using the data of a Mackerel-mimicking robot, with body rotation model,  $\phi_1 = 0.6\sin(4.0t)$ ,  $\phi_2 = 0.3\sin(4.0t - \pi/3)$ .

## 6 Conclusions

A mackerel-mimicking robot fish is fabricated to investigate the optimal motion pattern of a robotic fish. The hydrodynamic coefficients are obtained from the experimental study. Numerical simulator is developed based on the measured hydrodynamic coefficients. The optimal values of body shape parameters with low-energy consumption are obtained for a given magnitude of the propulsion force. Using the optimized body shape parameters, the propulsion force exerted on the front body of the robotic fish are expressed as a function of the Strouhal number.

Present study shows the possible application of the intelligent control of the robot fish. However, present results are only limited to the case of the robot fish stationed to a fixed place. Present method will be extended to the case of a maneuvering robot fish in the future.

## Acknowledgement

This research was supported by a grant from the University Restructuring Program (funded by the Ministry of Education and Human Resources Development) of Chungju National University.

## References

- [1] Gray J. Studies in animal locomotion VI. The propulsive powers of the dolphin. *Journal of Experimental Biology*, 1936, **13**, 192–199.
- [2] Fish F E, Lauder G V. Passive and active flow control by swimming fishes and mammals. *Annual Review of Fluids Mechanics*, 2006, **38**, 193–224.
- [3] Triantafyllou M S, Techet A H, Hover F S. Review of experimental work in biomimetic foils. *IEEE Journal of Oceanic Engineering*, 2004, **29**, 3.
- [4] Rozhdestvensky K V, Ryzhov V A. Aerohydrodynamics of flapping-wing propulsors. *Progress in Aerospace Sciences*, 2003, **39**, 585–633.
- [5] Bandyopadhyay P R. Trends in biorobotic autonomous undersea vehicles. *IEEE Journal of Oceanic Engineering*, 2005, **30**, 109–139.
- [6] Liu J D, Hu H S. A 3D simulator for autonomous robotic fish. *International Journal of Automation and Computing*, 2004, **1**, 42–50.
- [7] Lighthill M J. Note on the swimming of slender fish. *Journal of Fluid Mechanics*, 1960, **9**, 305–317.
- [8] Yu J Z, Wang L. Parameter optimization of simplified propulsive model for biomimetic robot fish. *Proceeding of the IEEE International Conference, Robotic and Automation*, Barcelona, Spain, 2005, 3306–3311.
- [9] Mason R. Fluid Locomotion and Trajectory Planning for Shape-Changing Robots. PhD Thesis. California Institute of Technology, USA, 2003.
- [10] Yu J Z, Liu L Z, Wang L. Dynamic modeling and experimental validation of biomimetic robotic fish. *Proceedings of the American Control Conference*, Minneapolis, Minnesota, USA, 2006, 4129–4134.